

# Thermal Effects on Cavitation Instabilities in Helical Inducers

Angelo Cervone\*

*Alta S.p.A., 56121 Pisa, Italy*

Renzo Testa†

*University of Pisa, 56100 Pisa, Italy*

Cristina Bramanti‡ and Emilio Rapposelli§

*Alta S.p.A., 56121 Pisa, Italy*

and

Luca d'Agostino¶

*University of Pisa, 56100 Pisa, Italy*

The main results of an experimental campaign conducted in the Cavitating Pump Rotordynamic Test Facility at Alta S.p.A. are presented. The experiments have been carried out on two different axial inducers (a three-bladed aluminum-made inducer of simple helical geometry and a prototype of the axial inducer of the Vulcain MK1 engine liquid oxygen turbopump) to characterize the instabilities affecting the pumps in a wide range of flow conditions; some experiments have also been carried out at higher temperatures to investigate the possible influence of the thermal cavitation effects on the observed phenomena. The transparent inlet section of the facility has been instrumented with several piezoelectric pressure transducers located at three axial stations: inducer inlet, outlet, and middle of the axial chord of the blades. For each axial station, at least two transducers were mounted at a given angular spacing to cross correlate their signals for coherence and phase analysis. The most interesting instabilities have been detected on the three-bladed inducer, including a cavitation surge, a rotating stall, and an auto-oscillation leading to a violent surge-mode instability. Some of these instabilities have also been found to be slightly affected by temperature. On the other hand, very few oscillating phenomena have been detected on the MK1 inducer, with a practically flat frequency spectrum at flow coefficients near its nominal operating point.

## Nomenclature

$c$	=	blade chord
$f$	=	frequency
$p_{in}$	=	inlet pressure
$p_v$	=	vapor pressure
$Q$	=	volumetric flow rate
$Re$	=	Reynolds number
$r_H, r_T$	=	inducer hub and blade tip radii
$s$	=	circumferential blade spacing
$T$	=	temperature
$\beta_T$	=	inducer tip blade angle
$\Delta p$	=	pressure rise caused by inducer
$\rho$	=	density
$\sigma$	=	cavitation number
$\phi$	=	flow coefficient
$\psi$	=	head coefficient
$\Omega$	=	rotational speed

## Introduction

IN space rockets, turbopumps used for propellant feeding are a crucial component of all primary propulsion concepts powered by liquid-propellant engines. Severe limitations are associated with the design of high power density, dynamically stable machines capable of meeting the extremely demanding suction, pumping, and reliability requirements of space transportation systems.<sup>1</sup> In most cases, these pumps employ an inducer upstream of the centrifugal stage(s) to improve the suction performance and reduce the propellant tank pressure and weight. Significant cavitation levels typically occur in inducers and often lead to the development of flow instabilities that can seriously degrade the performance of the machine, or even cause its rapid failure.

According to Brennen,<sup>2</sup> these flow instabilities can be divided in three main categories: global oscillations, local oscillations, and instabilities caused by radial or rotordynamic forces. Some of the most interesting and well-recognized instabilities in pumps and axial inducers are global oscillations, such as 1) rotating stall and rotating cavitation, propagating in the azimuthal direction at angular speeds different from that of the pump (typically subsynchronous for rotating stall and supersynchronous for rotating cavitation), and 2) surge and cavitation auto-oscillations, system instabilities involving strong flow and pressure oscillations of the whole suction line, typically occurring in noncavitating pumps for positive slopes of the characteristics (surge) and near breakdown conditions in cavitating turbopumps (cavitation auto-oscillations).

The occurrence of rotating cavitation has been extensively reported in the development of most high-performance liquid-propellant rocket fuel feed systems, including the U.S. space shuttle main engine, the European Ariane 5 engine, and the LE-7 of the H-II and H-II-A Japanese rockets. Together with cavitation surge, rotating cavitation is, therefore, becoming a major concern in modern highly loaded inducers, where both phenomena have been found to be caused by positive values of the pump's mass flow gain factor. Kamijo et al.<sup>3</sup> first reported a complete experimental characterization of azimuthal cavitation instabilities in axial inducers. They detected the occurrence of slightly supersynchronous rotating

Presented as Paper 2004-4021 at the AIAA/ASME/SAE/ASEE 40th Joint Propulsion Conference, Fort Lauderdale, FL, 11–14 July 2004; received 2 August 2004; revision received 1 February 2005; accepted for publication 7 February 2005. Copyright © 2005 by the American Institute of Aeronautics and Astronautics, Inc. All rights reserved. Copies of this paper may be made for personal or internal use, on condition that the copier pay the \$10.00 per-copy fee to the Copyright Clearance Center, Inc., 222 Rosewood Drive, Danvers, MA 01923; include the code 0748-4658/05 \$10.00 in correspondence with the CCC.

\*Project Manager, Via Gherardesca, 5, Ospedaletto; a.cervone@alta-space.com. Member AIAA.

†M.S. Student, Department of Aerospace Engineering; renzotesta@tiscali.it.

‡Project Engineer, Via Gherardesca, 5, Ospedaletto; c.bramanti@alta-space.com.

§Research Engineer, Via Gherardesca, 5, Ospedaletto; e.rapposelli@alta-space.com. Member AIAA.

¶Professor, Department of Aerospace Engineering; luca.dagostino@ing.unipi.it.

cavitation on a three-bladed inducer, leading to strong vibrations of the pump shaft at the same frequency, and suggested a simple modification of the pump housing to suppress this instability. Hashimoto et al.<sup>4</sup> analyzed in detail the influence of the number of blades, carrying out experiments on three- and four-bladed inducers. On both inducers, they detected the occurrence of cavitation surge, rotating cavitation, and steady asymmetric cavitation (a form of rotating cavitation with frequency exactly equal to the rotational speed of the pump and, therefore, appearing stationary with respect to the rotor blades). On the four-bladed inducer, they also observed a form of alternate blade cavitation, an instability similar to steady asymmetric cavitation and typical of inducers with an even number of blades, where two cavitation cells propagated synchronously at the pump rotational speed. Tsujimoto et al.<sup>5</sup> introduced the use of cross-correlation and phase analysis techniques in the experimental analysis of cavitation instabilities, to recognize oscillations of higher order characterized by a certain number of rotating cells. In the United States, Zoladz<sup>6</sup> carried out a series of experiments at the NASA Marshall Space Flight Center during the development of the liquid oxygen (LOX) turbopump of the Fastrac engine. An aluminum prototype of the inducer of this turbopump failed due to the strong oscillating stresses caused by cavitation surge and rotating cavitation. Recently, Tsujimoto and Semenov<sup>7</sup> identified in the LE-7 inducers a new high-order cavitation surge (axial) instability, occurring at frequencies as high as from four to five times the pump rotational speed and involving a periodic redistribution of cavitation along the blade channels, with no net change of the total cavitation volume. Contrary to conventional cavitation auto-oscillations, high-order cavitation surge is not, therefore, a system instability, as also suggested by its much higher frequency. According to the authors, its unforeseen resonance with the first bending mode of the inducer blades was responsible for the fatigue failure of the liquid hydrogen pump inducer of the eighth launch of the H-II rocket in November 1999.

A significant amount of work has also been developed for analyzing the various forms of flow instabilities in pumps by theoretical and/or numerical means.<sup>8–10</sup> In 2002 and 2003, d'Agostino and Venturini-Autieri<sup>11,12</sup> developed analytical models for the study of the rotordynamic forces on whirling axial and radial impellers, showing that internal resonances of the cavitating flow in the blade channels are likely to explain some of the main aspects of the observed spectral behavior of the lateral rotor forces caused by whirl motions of cavitating impellers.<sup>13,14</sup>

On the other hand, little experimental work has been carried out so far for investigating the influence of thermal cavitation effects on the onset and the development of flow instabilities caused by cavitation. Recent experiments carried out by the authors on a NACA 0015 hydrofoil in the Thermal Cavitation Tunnel at Centrospazio/Alta S.p.A., Pisa, Italy, have shown that both the amplitude and the stability limits of the various cavitation forms and instabilities observed on the foil strongly depend on the intensity of thermodynamic effects of the cavitating liquid.<sup>15</sup> Franc et al.<sup>16</sup> carried out a set of experiments on a four-bladed inducer in water and in R114 refrigerant fluid, finding two different cavitation instabilities: an alternate blade cavitation, affected by a thermal delay, and a rotating cavitation. The transition from alternate blade cavitation to rotating cavitation could not be correlated to a critical development of sheet cavities, and so it was supposed that tip-leakage cavitation plays an important role in the onset of rotating cavitation.

These findings naturally led to investigating to what extent thermal cavitation effects would affect flow instabilities in cavitating turbopumps. The present work illustrates the results of a number of experiments carried out to this end in the Cavitating Pump Test Facility (CPTF) at Alta S.p.A. on two different axial inducers over a wide range of operating conditions and water temperatures.

### Experimental Apparatus

The Cavitating Pump Rotordynamic Test Facility (CPRTF, Fig. 1) has been designed for experimental characterization of turbopumps in a wide variety of alternative configurations (axial, radial, or mixed flow, with or without an inducer).<sup>17</sup> The facility, operating in wa-



Fig. 1 CPRTF.

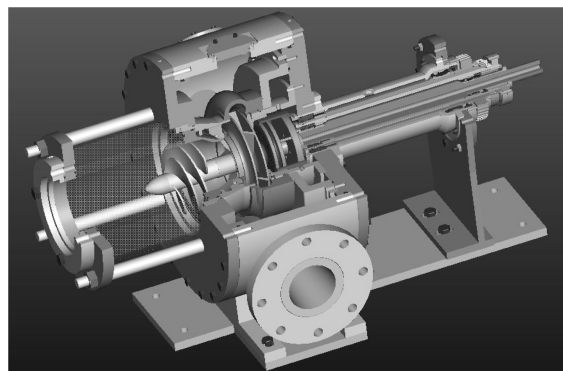


Fig. 2 Cutout of CPRTF test section.

ter at temperatures up to 90°C, is intended as a flexible apparatus that can readily be adapted to conduct experimental investigations on virtually any kind of fluid dynamic phenomena relevant to high-performance turbopumps. The test section (Fig. 2) is equipped with a rotating dynamometer for the measurement of the forces and moments acting on the impeller and with a mechanism for adjusting and rotating the eccentricity of the impeller axis in the range 0–2 mm and  $\pm 3000$  rpm. The inlet section, made of Plexiglas®, is transparent to allow for the optical visualization of the cavitation on the inducer.

For the present work, the facility has been assembled in its simplified CPTF configuration, without the rotating dynamometer and the adjustable eccentricity mechanism. To analyze the pressure fluctuations, the transparent Plexiglas inlet section (Fig. 3) has been instrumented with several flush-mounted piezoelectric pressure transducers located at three axial stations: inducer inlet, outlet, and middle of the axial chord of the blades. At each axial station at least two transducers were mounted with a given angular spacing to cross correlate their signals for coherence and phase analysis. As a result, waterfall plots of the power spectral density of the pressure fluctuations have been obtained and are shown as functions of the cavitation number  $\sigma = (p_{in} - p_v) / \frac{1}{2} \rho \Omega^2 r_T^2$  to identify the presence of flow instabilities in the flow conditions under consideration. Cross correlation of two pressure signals from different locations allowed determination of the axial or azimuthal nature of each instability and, in the second case, the number of rotating cells involved. All of the experiments were carried out maintaining a constant value of the flow coefficient and the pump rotational speed and gradually reducing the inlet pressure from atmospheric conditions to the minimum allowable value, at a constant rate of about 3 mbar/s.

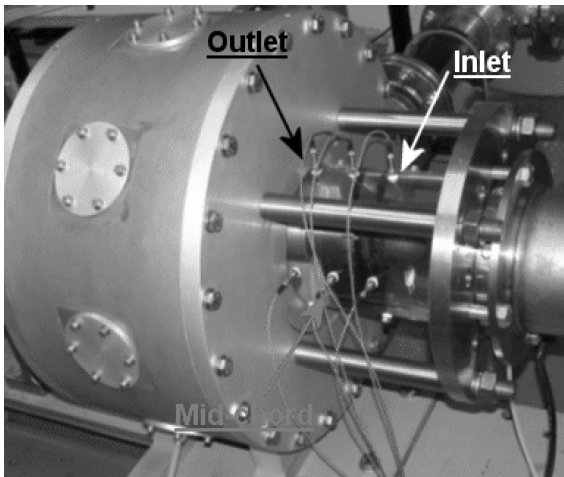


Fig. 3 Inlet section of facility with piezoelectric pressure transducers.

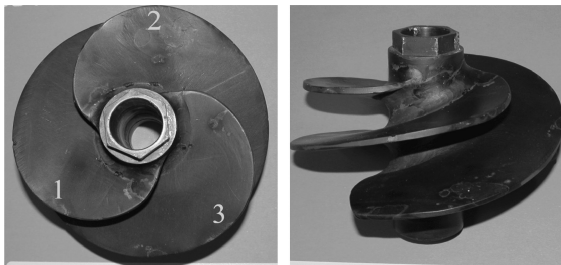


Fig. 4 FIP inducer.

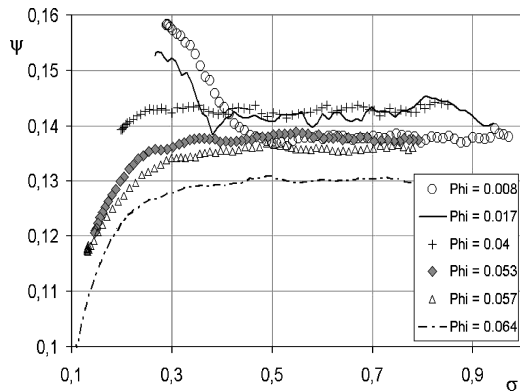


Fig. 5 Cavitating performance of FIP inducer.

### Test Inducers

Two different axial inducers have been used for the present experimentation. The first one (Fig. 4) is a three-bladed, aluminum-made inducer of extremely simple helical geometry, with a tip radius  $r_T = 81$  mm, a hub radius  $r_H = 22.5$  mm, a tip blade angle  $\beta_T = 9$  deg, a tip solidity  $c/s = 3.05$ , and 2-mm-thick backswept blades with blunt leading and trailing edges. It is manufactured by Fabbrica Italiana Pompe (FIP) S.p.A. for the food industry by welding the blades on the hub, and, therefore, it does not satisfy stringent geometric tolerances. The cavitating performance of this inducer, in terms of the head coefficient  $\psi = \Delta p / \rho \Omega^2 r_T^2$  as a function of the cavitation number  $\sigma$  for several values of the flow coefficient  $\phi = Q / \pi \Omega r_T^3$ , is shown in Fig. 5.

The second inducer used in the present experiments (Fig. 6) is a prototype of the inducer installed by Avio S.p.A. and installed in the LOX turbopump of the Ariane Vulcain MK1 rocket engine. It is a four-bladed axial inducer made of Monel alloy, with a tip radius  $r_T = 84$  mm; a profiled, variable-radius hub (36-mm inlet radius, 58-mm outlet radius); and backswept blades with sharp leading

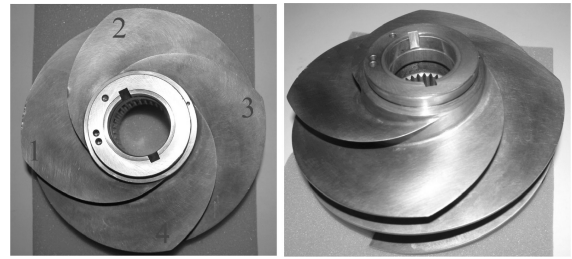


Fig. 6 MK1 inducer.

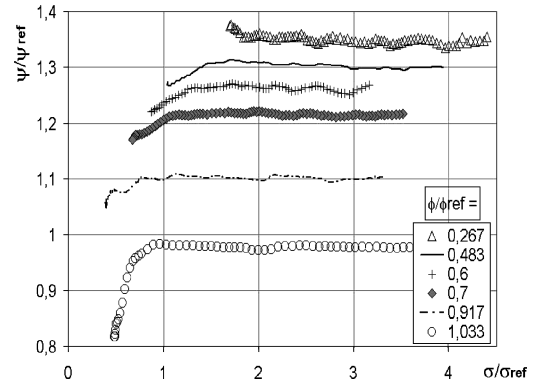


Fig. 7 Cavitating performance of MK1 inducer.

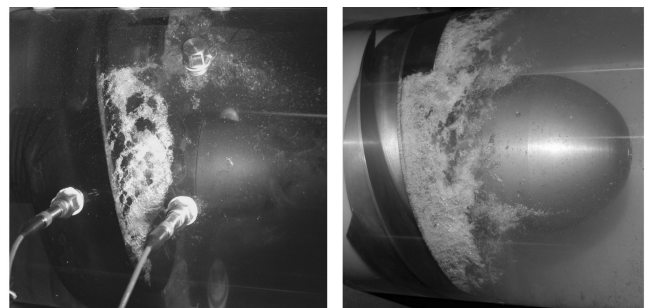


Fig. 8 Extensive cavitation in FIP inducer and in MK1 inducer.

edges, variable thickness, and nonuniform blade angle. The inlet tip blade angle is 7.7 deg, and the tip solidity is 2.1. The cavitating performance of the MK1 inducer is shown in Fig. 7, whereas Fig. 8 shows the two test inducers under heavy cavitating conditions. The experimental uncertainty indicated in Figs. 5 and 7 has been evaluated taking into account the random oscillations of the acquired data and the precision of the pressure transducers used for the experimentation.

Figures 5 and 7 show that, for lower flow coefficients, the inducer head is subject to a significant increase just before the breakdown. This phenomenon is particularly evident for the FIP inducer, but is also observable in the MK1: It is a well-known effect in axial pumps<sup>2</sup> due to an improved flow geometry associated, at low flow rates, with a modest amount of cavitation. Figure 5 also shows that, at the lower flow coefficients and higher cavitation numbers (non-cavitating conditions), the head-flow characteristic curve of the FIP inducer has a positive slope instead of the usual negative one.

### Results and Discussion

#### FIP Inducer

The tests on the FIP inducer have been carried out by mounting two piezoelectric transducers at each axial station, with a relative angular spacing of 90 deg. A wide range of flow coefficients has been investigated. Figures 9–12 show some typical results for the waterfall plots of the pressure fluctuation spectra measured at the inducer inlet section. The power spectral density and the phase and coherence function of the cross correlation between two pressure

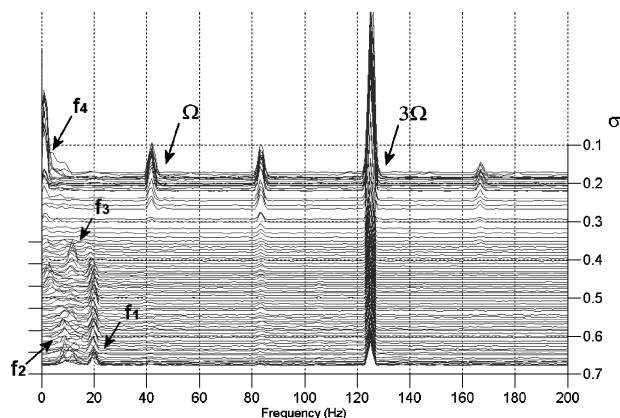


Fig. 9 Power spectrum of inlet pressure fluctuations in FIP inducer at  $\phi = 0.008$ , 2500 rpm, and room water temperature.

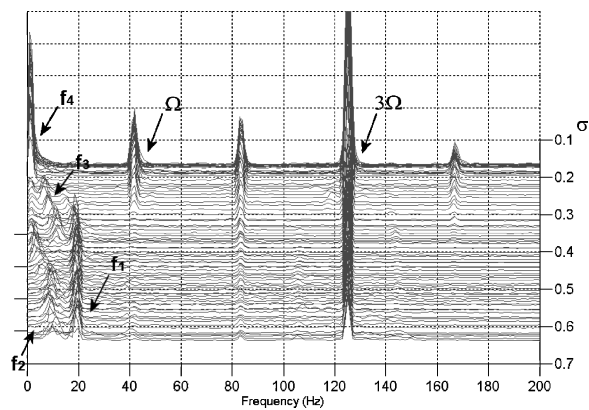


Fig. 10 Power spectrum of inlet pressure fluctuations in FIP inducer at  $\phi = 0.017$ , 2500 rpm, and room water temperature.

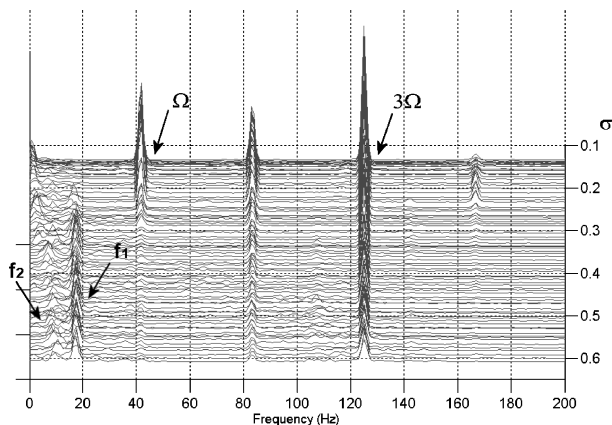


Fig. 11 Power spectrum of inlet pressure fluctuations in FIP inducer at  $\phi = 0.04$ , 2500 rpm, and room water temperature.

signals from the two transducers with 90-deg angular separation in the azimuthal direction at the inlet section of the inducer are illustrated in Figs. 13 and 14. Examination of these spectra shows the occurrence of five forms of instabilities, denoted by frequencies from  $f_1$  to  $f_5$ .

1) The frequency  $f_1$  is originated by a single-cell instability rotating in the circumferential direction. This conclusion has been drawn from the analysis of the cross correlation between the signals of the two piezoelectric transducers at the inlet station (Fig. 13), which showed a phase delay of about 90 deg (equal to the angular spacing between the transducers) with a value of the coherence function very close to unity. This instability, being subsynchronous, can probably be attributed to a form of rotating stall, probably associated with the positive slope of the head-rise performance curve (Fig. 5), whose

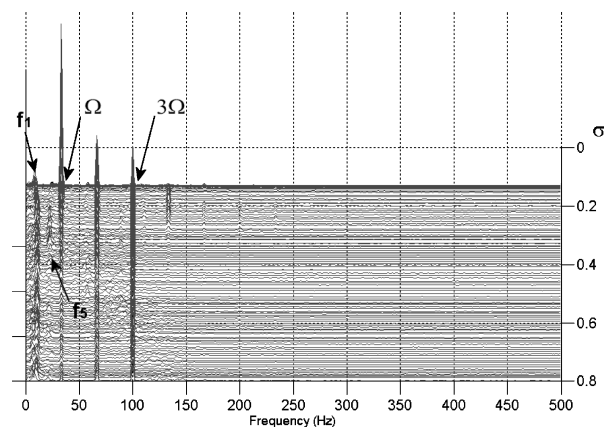


Fig. 12 Power spectrum of inlet pressure fluctuations in FIP inducer at  $\phi = 0.057$ , 2000 rpm, and room water temperature.

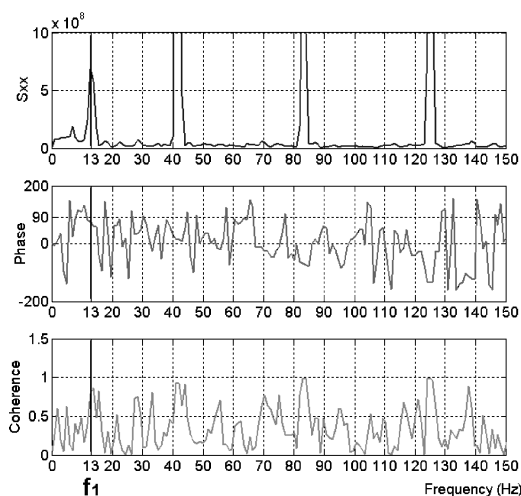


Fig. 13 Power density spectrum, phase delay, and coherence of pressure signals from two transducers with 90-deg angular separation in inlet section of FIP inducer ( $\phi = 0.057$ ,  $\sigma = 0.171$ , and  $\Omega = 2500$  rpm).

occurrence is facilitated by the blunt shape and rough finishing of the blade leading edges. Note that in the FIP inducer the geometry of the three blades is not exactly the same and can easily induce nonuniformities of the flowfield, forcing one blade to stall before the others and generating, even without cavitation, the asymmetric blockage typical of rotating instabilities. As a result, flow oscillations appear for practically every value of the flow coefficient, with a frequency of about  $0.34 \Omega$  that does not seem to depend on the presence of cavitation. The intensity of the instability decreases for very low values of  $\sigma$ , when the occurrence of generalized cavitation in the inducer inlet interferes with the fluctuations of the cavitation volume associated with the flow instabilities. Note that a similar result, characterized by the detection of rotating stall probably related to the occurrence of strong backflow in the inducer inlet, has been reported by Uchiyama et al.<sup>18</sup> during the development of the LE-7A liquid hydrogen pump.

2) The frequency  $f_2$  is related to a zeroth-order (axial) instability, as can be inferred from Fig. 14 because the cross correlation of the two pressure signals at the inlet station has a phase of 0-deg. This instability appears at all values of the flow coefficient with a frequency of about 9–11 Hz, slightly dependent on the flow coefficient and very close to the expected noncavitating natural frequency of the facility obtained from a linear one-dimensional model (Fig. 15). The instability at frequency  $f_2$  is, therefore, most likely due to the excitation of the natural mode of oscillation of the flow in the inlet line of the inducer.

3) The frequencies  $f_3$  and  $f_4$  are also due to axial instabilities. The first is a typical cavitation auto-oscillation, whose frequency tends

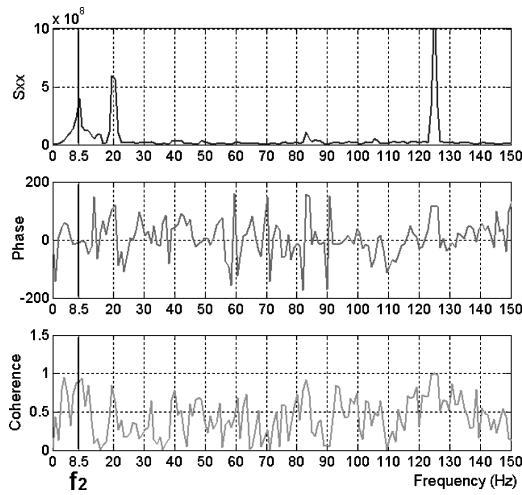


Fig. 14 Power density spectrum, phase delay, and coherence of pressure signals from two transducers with 90-deg angular separation in inlet section of FIP inducer ( $\phi = 0.008$ ,  $\sigma = 0.597$ , and  $\Omega = 2500$  rpm).

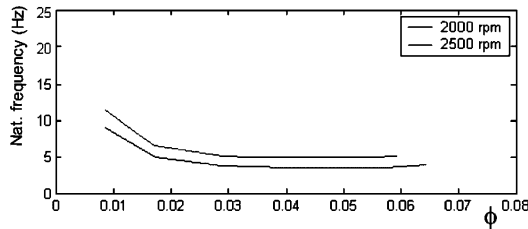


Fig. 15 Natural frequency of one-dimensional noncavitating axial flow oscillations in CPTF operating with FIP inducer at 2000 and 2500 rpm.

to decrease when the cavitation number is reduced, that is, for more extensive cavitation. At the lowest values of the flow coefficient and the cavitation number, this auto-oscillation leads to a surge (frequency  $f_4$ ) characterized by strong axial oscillations at very low frequency (about 1 Hz).

4) The frequency  $f_5$  appears only at the highest values of the flow coefficient and for moderately low values of the cavitation number (just before the occurrence of the breakdown). Examination of Figs. 13 and 14 indicates that it is an axial instability, probably sub-synchronous cavitation surge, with a frequency of about  $0.7 \Omega$ . Although this form of instability has often been reported to develop together with supersynchronous rotating cavitation, some researchers<sup>5</sup> have also observed it in the absence of supersynchronous phenomena, as in the present case.

Experiments have been also carried out at elevated temperature ( $T = 70^\circ\text{C}$ ) to analyze the influence of the thermal cavitation effects on cavitation-induced instabilities. The main results obtained from this study are summarized by the two waterfall plots presented in Figs. 16 and 17.

The most significant differences are related to the flow instabilities occurring with frequencies  $f_4$  (surge) and  $f_5$  (cavitation surge). Comparison of Figs. 9 and 16 shows that the strong oscillations caused by surge practically disappear at higher temperatures and lower flow coefficients, leading to a flatter spectrum at lower cavitation numbers. Similarly, comparison of Figs. 12 and 17 shows that cavitation surge oscillations (frequency  $f_5$ ) also tend to become less intense at higher temperatures, moving toward higher values of the cavitation number. The frequency of the oscillations, however, does not seem to depend on the water temperature.

No significant temperature-dependent variations have been found for the other instabilities, nor have any new oscillation phenomena been detected at higher temperatures. However, further experimental work is being carried on this matter, focusing, in particular, on how higher temperatures may change the dynamic behavior of the flow in cavitating inducers showing other forms of instabilities, such as rotating cavitation and high-order surge modes.

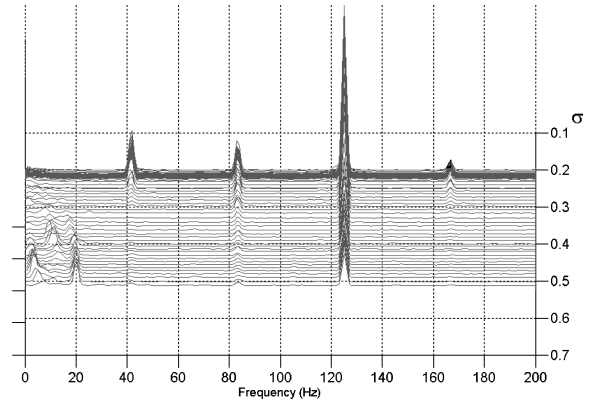


Fig. 16 Power spectrum of inlet pressure fluctuations in FIP inducer at  $\phi = 0.008$ , 2500 rpm pump rotational speed, and  $70^\circ\text{C}$  water temperature.

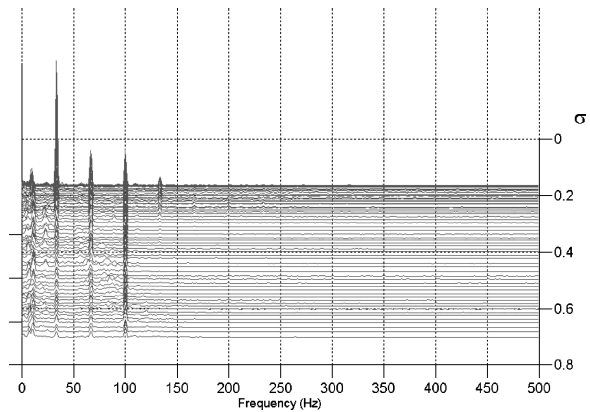


Fig. 17 Power spectrum of inlet pressure fluctuations in FIP inducer at  $\phi = 0.057$ , 2000 rpm pump rotational speed, and  $70^\circ\text{C}$  water temperature.

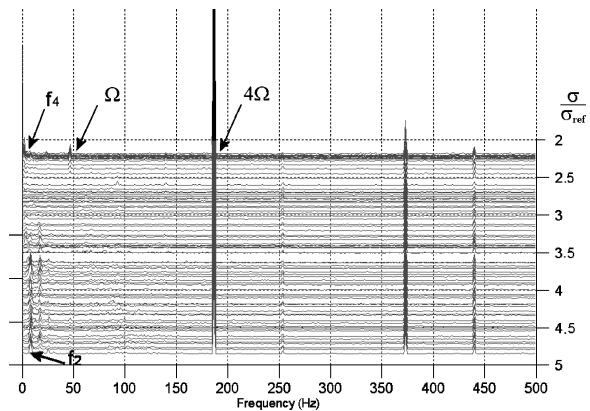
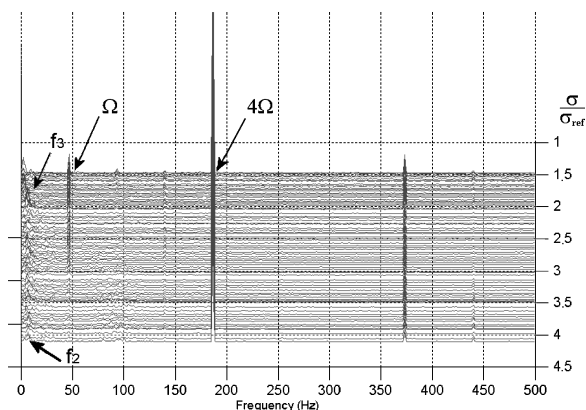


Fig. 18 Power spectrum of inlet pressure fluctuations in MK1 inducer at  $\phi/\phi_{\text{ref}} = 0.067$ , 2800 rpm pump rotational speed, and room water temperature.

#### MK1 Inducer

For the MK1 inducer, six piezoelectric transducers have been mounted at the inlet station, at an angular spacing of  $45^\circ$ , to better characterize the possible presence of rotating instabilities. The spectra of the pressure fluctuations measured on the MK1 inducer are presented in Figs. 18–20 and indicate that very few oscillation phenomena have been found. The only instabilities that have been observed are the natural mode of the facility at frequency  $f_2$  [with some multiples (Fig. 18) probably due to nonlinearity effects], an auto-oscillation  $f_3$ , and a very smooth surge  $f_4$ , with much less intense frequency peaks compared to those caused by the same



**Fig. 19** Power spectrum of inlet pressure fluctuations in MK1 inducer at  $\phi/\phi_{ref} = 0.383$ , 2800 rpm pump rotational speed, and room water temperature.

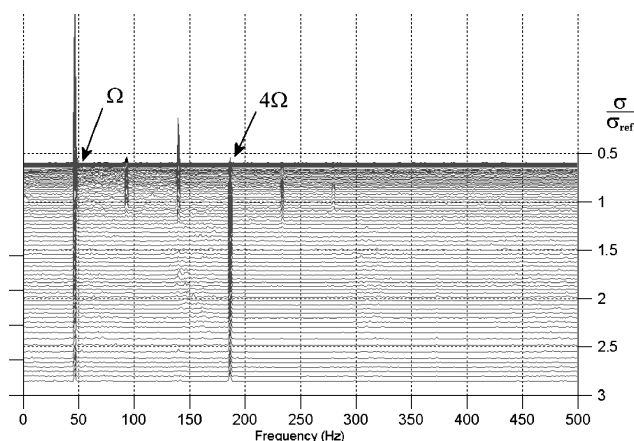


**Fig. 20** Power spectrum of inlet pressure fluctuations in MK1 inducer at  $\phi/\phi_{ref} = 1.067$ , 2800 rpm pump rotational speed, and room water temperature.

phenomenon on the FIP inducer. As in the case of the FIP inducer, the natural frequency is in good agreement with the value calculated using the linear one-dimensional model, whose results (Fig. 15) are slightly different in the two cases because of the different performance of the two inducers. At higher flow coefficients, near the nominal operating point of the MK1 inducer, the frequency spectrum becomes practically flat, except for the rotational frequency of the pump and its multiples (Fig. 20), thus confirming the effectiveness of the MK1 inducer design.

The instabilities for which an influence of the thermal effects has been detected on the FIP inducer are the surge and the cavitation surge. The first (surge) has been observed in a smooth form on the MK1 inducer, whereas the second (cavitation surge) has not been observed: For this reason, tests at elevated temperature have not been considered particularly useful in this case.

### Conclusions

A number of conclusions can be drawn from the experiments carried out in the CPRTF at Centropazio/Alta S.p.A. on two cavitating inducers operating with water at 20 and 70°C:

1) The combined use of the power spectrum, cross-correlation, phase, and coherence analysis of the flow pressure fluctuations measured at different locations on the shroud proved to be an effective technique for characterizing the nature and spatial configuration of the inducer flow instabilities.

2) The FIP helical inducer is more susceptible to developing cavitation-induced instabilities because of its simple design and rough manufacturing and shows the following flow instabilities: a) rotating stall, disappearing at very low values of the cavitation number and occurring at a frequency of about  $0.34 \Omega$ , which seems

to be independent on the presence and the extent of cavitation; b) the natural one-dimensional oscillation mode of the facility, whose frequency (9–11 Hz) is in good agreement with the value obtained from a simple linear one-dimensional dynamic model; c) cavitation auto-oscillation, whose frequency decreases at low cavitation numbers and tends to develop into a surge characterized by strong axial oscillations with a very low frequency (about 1 Hz) near shutoff conditions (very low values of the flow coefficient); and d) subsynchronous cavitation surge, with a frequency of about  $0.7 \Omega$ , which appears only at the highest values of the flow coefficient and for moderately low values of the cavitation number.

3) The MK1 inducer only showed evidence of a limited number of flow instabilities, namely, the natural mode of the facility, the cavitation auto-oscillation, and a very smooth cavitation surge.

4) At higher values of the flow coefficient, near its nominal operating point, the frequency spectrum of the Avio S.p.A. MK1 inducer becomes practically flat.

5) The thermal cavitation effects have a generally stabilizing effect on the onset of the observed cavitation-induced instabilities by significantly reducing the intensity of the pressure oscillations, but they do not appreciably change the frequency of the observed cavitation-induced instabilities, nor do they introduce significant new oscillation phenomena.

The results of the present initial set of experiments indicate that the influence of thermal effects on cavitation-induced flow instabilities in turbopump inducers is consistent with classical results for oscillating cavities, where thermal damping is known to increase rapidly with the liquid temperature. However, the presented data refer to a limited number of flow instabilities and frequencies, and, therefore, further experiments are needed to establish definitely the influence of thermal effects on cavitation-induced instabilities.

### Acknowledgments

The Cavitating Pump Test Facility and Cavitating Pump Rotor-dynamic Test Facility have been funded by the Agenzia Spaziale Italiana under the 1998 and 1999 contracts for fundamental research. The authors would like to thank Mauro Varetto of Avio S.p.A. for his kind assistance and express their gratitude to Mariano Andrenucci and Renzo Lazzeretti of the Dipartimento di Ingegneria Aerospaziale, Università di Pisa, for their constant and friendly encouragement.

### References

- <sup>1</sup>Stripling, L. B., and Acosta, A. J., "Cavitation in Turbopumps—Part 1," *Journal of Basic Engineering*, Vol. 84, Sept. 1962, pp. 326–338.
- <sup>2</sup>Brennen, C. E., *Hydrodynamics of Pumps*, Concepts ETI, Inc., Norwich, VT, and Oxford Univ. Press, Oxford, England, U.K., 1994.
- <sup>3</sup>Kamijo, K., Yoshida, M., and Tsujimoto, Y., "Hydraulic and Mechanical Performance of LE-7 Liquid Oxygen Pump Inducer," *Journal of Propulsion and Power*, Vol. 9, No. 6, 1993, pp. 819–826.
- <sup>4</sup>Hashimoto, T., Yoshida, M., Watanabe, M., Kamijo, K., and Tsujimoto, Y., "Experimental Study of Rotating Cavitation of Rocket Propellant Pump Inducers," *Journal of Propulsion and Power*, Vol. 13, No. 4, 1997, pp. 488–494.
- <sup>5</sup>Tsujimoto, Y., Yoshida, Y., Maekawa, Y., Watanabe, S., and Hashimoto, T., "Observation of Oscillating Cavitation of an Inducers," *Journal of Fluids Engineering*, Vol. 119, Dec. 1997, pp. 775–781.
- <sup>6</sup>Zoladz, T., "Observations on Rotating Cavitation and Cavitation Surge from the Development of the Fastrac Engine Turbopump," AIAA Paper 2000-3403, July 2000.
- <sup>7</sup>Tsujimoto, Y., and Semenov, Y. A., "New Types of Cavitation Instabilities in Inducers," 4th International Conf. on Launcher Technology, Centre National d'Etudes Spatiales, Paris, Paper 80, Dec. 2002.
- <sup>8</sup>Kamijo, K., Shimura, T., and Tsujimoto, Y., "Experimental and Analytical Study of Rotating Cavitation," *Cavitation and Gas-Liquid Flow in Fluid Machinery and Devices*, edited by T. J. O'Hern, J. H. Kim, W. B. Morgan, and O. Furuya, Vol. 190, American Society of Mechanical Engineers, 1994, pp. 33–43.
- <sup>9</sup>Tsujimoto, Y., Watanabe, S., and Horiguchi, H., "Linear Analyses of Cavitation Instabilities of Hydrofoils and Cascades," Proceedings of the U.S.–Japan Seminar: Abnormal Flow Phenomena in Turbomachinery, Osaka Univ., Japan, Nov. 1998.

<sup>10</sup>Tani, N., and Nagashima, T., "Numerical Analysis of Cryogenic Cavitating Flow on Hydrofoil—Comparison Between Water and Cryogenic Fluids," 4th International Conf. on Launcher Technology, Centre National d'Etudes Spatiales, Paris, Paper 27, Dec. 2002.

<sup>11</sup>d'Agostino, L., and Venturini-Autieri, M. R., "Three-Dimensional Analysis of Rotordynamic Fluid Forces on Whirling and Cavitating Finite-Length Inducers," 9th International Symposium on Transport Phenomena and Dynamics of Rotating Machinery (ISROMAC-9), Pacific Center of Thermal Fluids Engineering, USA and Osaka Univ.—Engineering Science, Japan, Paper FD-103, Feb. 2002.

<sup>12</sup>d'Agostino, L., and Venturini-Autieri, M. R., "Rotordynamic Fluid Forces on Whirling and Cavitating Radial Impellers," CAV 2003, 5th International Symposium on Cavitation, Japanese Ministry of Education, Culture, Sports, Science and Technology, and Hatakeyama Culture Foundation, Paper OS-4-002, Nov. 2003.

<sup>13</sup>Franz, R., Acosta, A. J., Brennen, C. E., and Caughey, T. K., "The Rotordynamic Forces on a Centrifugal Pump Impeller in the Presence of Cavitation," *ASME Journal of Fluids Engineering*, Vol. 112, No. 3, 1990, pp. 264–271.

<sup>14</sup>Bhattacharyya, A., Acosta, A. J., Brennen, C. E., and Caughey, T. K., "Rotordynamic Forces in Cavitating Inducers," *Journal of Fluids Engineering*, Vol. 119, No. 4, 1997, pp. 768–774.

<sup>15</sup>Rapposelli, E., Cervone, A., Bramanti, C., and d'Agostino, L., "Thermal Cavitation Experiments on a NACA 0015 Hydrofoil," 4th ASME-JSME Joint Fluids Engineering Conf., American Society of Mechanical Engineers, Paper FEDSM 2003-45006, July 2003.

<sup>16</sup>Franc, J. P., Rebattet, C., and Coulon, A., "An Experimental Investigation of Thermal Effects in a Cavitating Inducer," CAV 2003, 5th International Symposium on Cavitation, Japanese Ministry of Education, Culture, Sports, Science and Technology, and Hatakeyama Culture Foundation, Paper GS-16-001, Nov. 2003.

<sup>17</sup>Rapposelli, E., Cervone, A., and d'Agostino, L., "A New Cavitating Pump Rotordynamic Test Facility," AIAA Paper 2002-4285, July 2002.

<sup>18</sup>Uchiumi, M., Kamijo, K., Hirata, K., Konno, A., Hashimoto, T., and Kobayashi, S., "Improvement of Inlet Flow Characteristics of LE-7A Liquid Hydrogen Pump," AIAA Paper 2002-4161, July 2002.